Laser-Induced Breakdown Spectroscopy: Application to Nuclear Waste Management -- 9166

Seong Yong Oh, Fang Yu Yueh, Jagdish P. Singh*

Institute for Clean Energy Technology
Mississippi State University, Starkville, MS 39759, USA

Kristine E. Zeigler

Savannah River National Laboratory, Aiken, SC 29808, USA

ABSTRACT

Laser-induced breakdown spectroscopy (LIBS) was applied to the analysis of simulant slurry samples used in the vitrification process of liquid radioactive wastes. The capability of direct analysis of slurry will significantly increase analytical throughput and will reduce waste generation in radiological analytical facilities, providing analyses suitable for waste acceptance and production records. LIBS as a remote and the real-time analytical tool has been evaluated for direct analysis of the Defense Waste Processing Facility (DWPF) Sludge Receipt and Adjustment Tank (SRAT) product. This paper examines the experimental conditions associated with the slurry measurement with LIBS to achieve good measurement precision. LIBS analysis was performed by two different detection systems: Czerny-Turner spectrometer coupled with intensified diode array detector (IDAD) and an Echelle spectrometer with intensified charge coupled device (ICCD). The Echelle detection system shows a high efficiency in simultaneous multi-element detection and determination of the physical quantities of the simulant.

INTRODUCTION

Laser induced breakdown spectroscopy (LIBS) is the spectroscopic method which analyzes the elemental composition in a laser-produced plasma plume which is produced by a focused high pulse energy laser beam. Strong electric field of laser pulse and pulse-duration induce the ablation, atomization, ionization and excitation of the sample. The spectral information which reflects the existence of the characteristic atom in the sample can be obtained from these optical emission spectra. LIBS is suitable for rapid on-line elemental analysis of any material phase and has proved its value in obtaining analytical atomic emission spectra directly from solid, liquid, and gaseous samples.[1-3] LIBS is a fast qualitative analysis technique that has been used on a variety of samples such as polluted soils, Mars surface, alloy, glass, explosive, tissues, etc. In some solid samples, LIBS has demonstrated an accuracy of 3-6% for elements with a concentration greater than 1 wt% and an accuracy of 5-10% or better for minor elements depending on their concentration.[4,5]

Recently, LIBS technique has been popular because of its intrinsic advantages and the significant developments of instrument (broadband spectrometer with high resolution and intensified charge coupled device). Conjugation with the optical fiber, minimal sample preparation, and quick on-line elemental analysis are the distinguishable marks of the LIBS probe, which make it practicable to apply in the inaccessible place.[6,7] The typical laboratory analytical tools are generally unsuitable for field application. For example, ICP require the dissolution of sample to spray into a flame as a form of an aerosol. In the other hand, LIBS technique has ability to direct detection that can reduce time involved in sample pretreatment processes. Moreover, fast direct analysis and availability of optical fiber can avoid

the risk of hazardous reagents and contamination of sample. LIBS technique can analyze conducting as well as non-conducting material because of the use of the laser beam.
Vitrification of liquid radioactive wastes is an essential task in nuclear industries, facilitating the safe handling and long-term storage of radioactive waste. Analytic tools are necessary for analyzing the sludge prior to and during the vitrification process of the liquid radioactive wastes. The LIBS technique has been applied for the analysis of glass [8], glass melts [9,10] and glass batch [11]. The aim of this paper is to explore the possibility of applying LIBS as a remote and the near real-time analytical tool that can be used to analyze liquid radioactive wastes during the vitrification process using two detection systems. The main issues to be resolved with LIBS analysis of liquid samples are poor detection sensitivity and precision. Because water can quench the laser plasma and suppresses the LIBS signal, poor sensitivity may result. Large standard deviations for LIBS liquid data are due to the laser induced shock wave caused turbulence on the liquid surface. Slurry samples contain a large amount of water and large particle sizes. The effects of water content and particle sizes on LIBS measurement will also need to be studied to determine best data analysis method. To evaluate the figure of merit of direct slurry measurement with LIBS, two DWPF simulant slurry samples with different acid levels from SRNL were used in the study. The test results with these slurry samples showed that the splattering and surface cavitations result in large signal fluctuation. To improve LIBS' reproducibility and detection limits for slurry measurements, various experimental parameters which can affect LIBS' analytical figure of merit were studied. The study has shown that by using the appropriate slurry sample handling systems, optimum experimental parameters and some data processing techniques, reasonable accuracy and precision for the major elements can be achieved.[12] However, further work on improving signal sensitivity and data reproducibility is needed. The Echelle detection system providing broadband with high resolution is more suitable for detecting the multiple elements than the Czerny-Turner detection system for the application of the LIBS technique [11,13]. The work presents the results of LIBS analysis of simulant slurry samples using two different detection systems: Czerny-Turner spectrometer coupled with intensified diode array detector (IDAD) and an Echelle spectrometer with intensified charge coupled device (ICCD).

2. EXPERIMENTAL DETAILS

2.1 LIBS Systems

Two different systems based on Czerny-Turner and Echelle spectrometers have been applied to record the LIBS spectra in this study (See Table 1 for the specification of these two detection systems). Figure 1 shows a general schematic diagram of the experimental setup used for recording LIBS spectra. A frequency-doubled, Q-switched Nd:YAG laser (Continuum Surelite I for the Czerny-Turner and Continuum Surelite III for the Echelle detection system) was incorporated into the LIBS system as an excitation source. The 532-nm laser light is focused onto the sample surface using an ultraviolet (UV) grade quartz lens of 300 or 500 mm focal length. Atomic emission from the laser-induced plasma was collected by an optical fiber bundle using a UV-grade quartz lens. The first detection system contains a Czerny-Turner spectrograph (SPEX 500M) with a grating of 2400 grooves/mm fitted with a 1024-element intensified diode array detector (IDAD). The simultaneous spectral coverage of this detection system is about 20 nm with a linear dispersion of 19.5 pm/pixel. The Echelle spectrometer detection system is equipped with a 1024 x 1024 element intensified charge coupled device (ICCD). The simultaneous spectral coverage of this detection system is from 200-780 nm. The linear dispersion for the Echelle spectrometer system varies from 5 pm/pixel at 200 nm to 19 pm/pixel at 780 nm. Therefore, the Echelle spectrometer detection system provides a higher resolution capability at the UV-VIS region than the Czerny-Turner spectrometer system. A pulse generator is used to trigger and synchronize the detector with the laser operation and provides the desired gate delay and width for detection. Figure 2 shows a spectral comparison of the LIBS signal recorded by the Czerny-Turner spectrometer and the Echelle spectrometer, respectively. The Czerny-Turner spectrometer has a linear dispersion value greater than that

of the Echelle spectrometer [11] at the observed spectral region and therefore, it is not sufficient to resolve the multiple spectral emission lines in the region shown in Figure 2.

2.2 Sample Preparation

Sludge Receipt and Adjustment Tank (SRAT) slurry sample used in this study is mainly made up of 78.2% water (H_2O), 5.8% ferric oxide (Fe_2O_3), 2.6% alumina (Al_2O_3), 3.6% sodium oxide (Na_2O), and small quantities of oxides of carbon, silica, chromium, manganese, magnesium, etc. The slurry composition was chosen as a surrogate for the radioactive slurry that is input into the Savannah River Site's Defense Wastes Processing Facility (DWPF) glass melter. For the vitrification process, the slurry sample was first acidified until the pH 6 using strong nitric acid. Glass frit containing SiO_2 (70.0%), B_2O_3 (12.0%), Na_2O (11.0%), Li_2O (5.0%) and MgO (2.0%) was added into the acidified SRAT slurry. This mixture called as the slurry mix evaporator (SME) products is finally fed into the glass melter to make the solid stimulant low activity test reference material (LRM) glass.

3. RESULTS AND DISCUSSIONS

3.1 Characteristics of laser-induced plasma

Echelle spectrometer provides large spectral coverage (200-780nm) with good spectral resolution, it is therefore used to characterize laser-induced plasma from slurry sample. The integrated emission line intensity in the optically thin plasma condition is given by

$$I = B\frac{hc}{\lambda}A_{ji}g_j\frac{n_x \exp(-E_j/kT)}{U(T)} \qquad (1)$$

Here, n is the total number density of species x, T is the excitation temperature, U(T) is the atomic partition function, λ is the transition wavelength (in m). h is Planck's constant (in Js), c is the speed of light (in m/s), B is a constant factor, A_{ji} is the transition probability (in s^{-1}), the index j-th and i-th indicate the upper and lower atomic levels, and g_j is the degeneracy of the upper atomic level. The excitation temperature can be calculated for the same species [14] by the natural logarithm of Equation (1):

$$\ln\frac{I\lambda}{A_{ji}g_j} = \ln\left(\frac{n_x}{U(T)}\right) - \frac{E_j}{kT} \qquad (2)$$

This method is known as Boltzmann plot and uses the slope of the dashed line (-1/kT), obtained from linear fitting, to yield the excitation temperature. The excitation temperature was also estimated from Fe I line intensities of SME products as a function of Fe concentrations. The average excitation temperature was 7137K. The error bars in the excitation temperature correspond to the standard deviation of ten measurements [15]. The spectral line wavelengths, energies of the upper levels, statistical weights, and transition probabilities for each element were obtained from NIST atomic spectral database [16].

Electron density can be estimated by the Stark broadened FWHM linewidth, based on the electron impact approximation, and corrected for quasi-static ion broadening [17]. Assuming the contribution from quasi-static ion broadening to be negligible, the ratio formulation for non-hydrogen-like emission lines is given by

$$\frac{\Delta\lambda_{Stark}}{n_e} \approx \left(\frac{2w_e}{10^{16}}\right) \qquad (3)$$

Here, $\Delta\lambda_{Stark}$ is the Stark broadened FWHM linewidth in Angstrom, n_e is the electron density in cm^{-3}, and w_e is the reference electron impact parameter width in Angstrom. The constant (10^{16}) in cm^{-3} is the reference electron density. Notably, Stark broadened FWHM ($\Delta\lambda_{Stark}$) is the main contribution of Lorentz

broadening FWHM linewidth (i.e. $\Delta\lambda_{Stark} \approx \Delta\lambda_L$) [18]. Considering the symmetry of the observed emission line centered at the peak value, the Fe I line at 381.584 nm was selected to extract the FWHM linewidth of the Lorentz component ($\Delta\lambda_L$). A non-linear least-squares fitting of Voigt function to the observed experimental data points ,obtained from the SME product with 4.05% Fe concentration, was performed utilizing a Levenberg-Marquardt algorithm installed in Origin software version 7.0 (OriginLab Co., USA). The estimated electron density was 2.06×10^{16} cm^{-3} using the calculated Lorentz linewidth. Substituting the electron density in equation (4) yielded the ionization temperature [19,20] which was estimated as 7120K from Fe I 381.584 nm and Fe II 275.574 nm :

$$\frac{I_{ion}}{I_{atom}} = \frac{2(2\pi m_e kT_{ion})^{\frac{3}{2}}}{n_e h^3}\left(\frac{gA}{\lambda}\right)_{ion}\left(\frac{\lambda}{gA}\right)_{atom}\exp\left(-\frac{V^+ + E_{ion} - E_{atom}}{kT_{ion}}\right) \qquad (4)$$

Here, I_{atom} (I_{ion}) is the integrated emission intensity of the atom (ion), V^+ is the ion potential of the atom, E_{ion} is the excited level energy of the ionic line, and E_{atom} is the excited level energy of the atomic line. T_{ion} is ionization temperature. The calculation was performed repeatedly until the relative error between the calculated n_e (Eq. 3) and estimated n_e (Eq. 4) was found below 1% [19]. The validity of the LTE assumption can be evaluated by the following the equation from the electron density and excitation temperature [21]:

$$n_e >> 1.6\times10^{18} T^{1/2}\Delta E^3 \qquad (5)$$

where T is in K, ΔE is in eV, and n_e is in m^{-3}. Here, ΔE is the largest energy gap for the identified element. ΔE is under 3.3 eV and the lower limit for n_e was estimated to be $0.45\times10^{+16}cm^{-3}$.

3.2 Slurry Calibration with Normalization Intensity by Czerny-Turner Spectrometer System

Normalized intensity is defined as the ratio of the atomic emission line area intensity to the released whole plasma emission area intensity [22,23]. The whole plasma emission area intensity was calculated by integrating of a selected spectral region covering ~20 nm. The atomic emission line intensity of Fe I 382.043 nm transition with and without the normalization which is obtained from ten measurements of an average of 360 laser shots repeated over an extended period of 7 days. For the Fe I 382.043 nm atomic emission line, the averaged relative standard deviation (RSD) values of intensity was ~34.74%. But with plasma emission normalization the averaged RSD values was improved significantly to 5.92%. The laser shot-to-shot fluctuation has contributed to LIBS's poor reproducibility. Fe I 382.043 nm and Al I 394.403 nm atomic emission line intensities were recorded at different laser energies. The two atomic emission line intensities clearly vary linearly with laser energy in the range 70 to 110mJ per pulse. The signal saturation, which can be expected at the higher laser energy which was not observed in this laser pulse energy range. Meanwhile, the normalized intensity was insensitive to variations in laser energy in the 70 to 110 mJ per pulse range. The RSD values of the normalized intensities of Fe I 382.043 nm and Al I 394.403 nm were calculated to be 3.6 % and 3.4 %, respectively. These analysis results shows that we can improve the measurement reproducibility with plasma emission normalization.

Calibration curves were created using data from the SRAT slurry with the addition of varying quantities of Fe_2O_3 and Na_2CO_3 (see Fig. 3). For comparison, the calibration data based on plasma emission normalization were also shown in Fig. 3. We found that the normalized intensity not only allows the application of the calibration curve but provides an improved correlation coefficient of the calibration curve.

3.3 Slurry Calibration with Echelle Spectrometer System

For calibration curve generation using the Echelle spectrometer system, slurry sample with varying compound concentrations were prepared by adding glass frit (12% B_2O_3, 5% Li_2O, 11% Na_2O, 2% MgO and 70% SiO_2 %) into acidified SRAT slurry. The strong doublet resonance line of lithium (Li) at 670.7

nm, which is prone to the self-absorption effect was found to be linear with increasing Li concentration (wt %). In contrast, the intensity of atomic Si I 288.158 nm, was much weaker in the spectra (see Fig. 4.a). This may be due to the sedimentation of glass frit because of its weight. Sedimentation in the LIBS analysis can be an obstacle because the plasma is created on the surface.

To overcome this potential issue, two ideas were explored. We have added fine silicon dioxide powder (SiO_2) to the slurry sample instead of the glass frit. Also, the spectral response of each atomic emission line can be optimized with gate delay time. After preparing the slurry sample containing 3.5 wt% Si, the gate delay time was varied from 300 ns to 3000 ns at a fixed 80 mJ/pulse laser energy. We observed the Si I 288nm intensity rapidly decay with the increase in gate delay time. The more sensitive calibration curve of silicon was obtained using a shorter gate delay time (300 ns) and higher laser energy (80 mJ/pulse) (see Fig. 4.b). The linearity and spectral response of Si I 288.158 nm were clearly improved as compared with the data from slurry sample that have been taken by addition of different amount of glass frit. LOD (Limit of detection) values of Si I 288.158 nm were calculated by using $LOD = \sigma_B/S$, where σ_B is the standard deviation of the background and S is the slope of the calibration curve. LOD values obtained from slurry sample mixed with glass frit and slurry sample mixed with finer silicon dioxide powder (SiO_2), were estimated to be 0.51 wt% and 0.043 wt%, respectively. However, using the parameters of short gate delay and high laser power led to the saturation of the strong emission lines of other elements. For example, the signal saturation of the Ca II 393.365 nm transition was observed using a 300 ns gate delay time and 80mJ/pulse laser energy.

4. CONCLUSIONS

The capabilities of in-situ and remote analysis in the LIBS technique make it a good candidate as an analytic tool for evaluating liquid radioactive wastes during the cycles of the vitrification process. The LIBS technique can become a very popular analytical tool if the reliability of its quantitative analysis significantly improves. We observed that the normalization method improves the reproducibility of LIBS signals. The LIBS measurement of slurry samples includes the intrinsic challenge of sedimentation. The homogenous distribution of all elemental compositions in the liquid sample is essential to get accurate LIBS signals. In the case of the glass frit, the lower spectral response at Si I 288.158 nm was observed because of its sedimentation. Spectroscopic analysis using the Echelle detection system is more efficient for simultaneous multi-element detection. However, it is important to carefully select the experimental parameters, such as gate delay and laser power to avoid saturation of strong emission lines.

ACKNOWLEDGEMENT

Authors would like to thank T. Miller for assistance in laboratory and David Peeler for discussion during the work. This work is funded by U.S. Department of Energy (DOE) Cooperative Agreement No. DE-FC01-06EW07040.

REFERENCES

1. “Laser Induced Breakdown Spectroscopy” Editors Jagdish P Singh and S. N. Tahkur, (Elsevier, Amsterdam, 2007).

2. Fang-Yu Yueh, Jagdish P. Singh and Hansheng Zhang, "Laser-induced breakdown spectroscopy-elemental analysis", in Encyclopedia of Analytical Chemistry, R. A. Meyers, ed. (Wiley, New York, 2000).

3. A. Miziolek, I. Schechter and Peleschi, "Laser induced plasma spectroscopy: , a review of recent advances, " Rev. Anal. Chem. 16, 173-298 (1997).

4. B. Lal, F. Y. Yueh, J. P. Singh, "Glass-batch composition monitoring by laser-induced breakdown spectroscopy", Appl Opt. 44, 3668-74 (2005).

5. H. Zheng, F. Y. Yueh, T. Miller, J. P. Singh, K. Zeigler and J. Mara, "Analysis of Surrogate of Plutonium (Pu) Residue Using Laser Induced Breakdown Spectroscopy", Spectrochimica Acta 63, 968-974 (2008).

6. U. Panne, R.E. Neuhauser, C. Haisch, H. Fink, and R. Niessner, "Remote Analysis of a Mineral Melt by Laser-Induced Plasma Spectroscopy," Appl. Spectro., 56, 375, (2002).

7. A.I. Whitehouse, J. Young, I.M. Botheroyd, S. Lawson, C.P. Evans and J. Wright, "Remote material analysis of nuclear power station steam generator tubes by laser-induced breakdown spectroscopy," Spectrochim. Acta Part B 56, 821-830 (2001).

8. C. F. Su, S. Feng, J.P. Singh, F.Y. Yueh, J.T. Rigby, D.L. Monts , R.L.Cook, "Glass Composition Measurement Using Laser Induced Breakdown Spectrometry," Glass Technol. 41, 16-21 (2000).

9. J.I. Yun, R. Klenze, J.I. Kim, "Laser-Induced Breakdown Spectroscopy for the On-Line Multielement Analysis of Highly Radioactive Glass Melt. Part I: Characterization and Evaluation of the Method," Appl. Spectrosc. 56, 437-448 (2002).

10. U. Panne, C. Haisch, M. Clara, R. Niessner, "Analysis of glass and glass melts during the vitrification process of fly and bottom ashes by laser-induced plasma spectroscopy. Part I. Normalization and plasma diagnostics," Spectrochim. Acta Part B 53 (1998) 1957–1968.

11. B. Lal, .F.Y. Yueh, and J.P. Singh, "Glass batch composition monitoring by laser induced breakdown spectroscopy," Appl. Opt. 44 (2005) 3668-3674.

12. S.Y. Oh, T. Miller, F. Y. Yueh, and J. P. Singh, "Comparative study of laser induced breakdown spectroscopy using two slurry circulation systems", Applied Optics 46, 4020-4025 (2007).

13. H. E. Bauer, F. Leis, K. Niemax, "Laser Induced Breakdown Spectrometry with an Echelle Spectrometer and Intensifier Charge Coupled Device Dectection," Spectrochim. Acta. Part B. 53, 1815-1825 (1998).

14. M. Sabsabi, P. Cielo, "Quantitative Analysis of Aluminum Alloys by Laser-Induced Breakdown Spectroscopy and Plasma Characterization," Appl. Spectrosc. 49 499-507 (1995).

15. Yonung-ik Sung, H.B. Lim, "Plasma temperature measurement of a low-pressure inductively coupled plasma using spectroscopic method," J. Anal. At. Apectrom, 18, 897-901 (2003).

16. National Institute of Standards and Technology, U.S.A., Electronic Database, http://physics.nist.gov/PhysRefData/ASD/lines_form.html

17. G. Bekefi, "Principle of Laser Plasmas", John Wiley & Sons, New York, 1976.

18. C. Wang, F. J. Mazzotti, S. P. Koirala, C. B. Winsted, G. P. Miller, "Measurments of OH Radical in a Low-power Atmospheric Inductively Coupled Plasma by Cavity Ringdown Spectroscopy," Appl. Spectro. 734-740 (2004).

19. V. Detalle, R. Heon, M. Sabsabi, L. St-Onge, "An evaluation of a commercial Echelle spectrometer with intensified charge-coupled device detector for materials analysis by laser induced plasma spectroscopy," Spectrochim. Acta. Part B. 56 1011-1025 (2001).

20. O. Smaek, D. C. S. Beddows, J. Kaiser, S. V. Kukhlevsky, M. Liska, H. H. Telle , J. Young, "Application of Laser Induced Plasma Spectroscopy to In Situ Analysis of Liquid Samples," Opt. Eng. 39 2248-2262 (2000).

21. A. Thorne, U. Litzen, S. Johansson, "Spectrophysics: Principles and Applications" , Springer New York, 1999, pp. 170-223.

22. J.-B. Sirven, B. Bousquet, L. Canionl, and L. Sarger, "Laser Induced Breakdown Spectroscopy of Composition Samples: Comparison of Advanced Chemometrics Methods," Anal. Chem. 78, 1462-1469 (2005).

23. V. Lazic, R. Fantoni, F. Colao, A. Santagata, A. Morone, V. Spizzichino, "Quantitative laser induced breakdown spectroscopy analysis of ancient marbles and corrections for the variability of plasma parameters and of ablation rate," J. Anal. At. Spectrom. 19, 429-436 (2004).

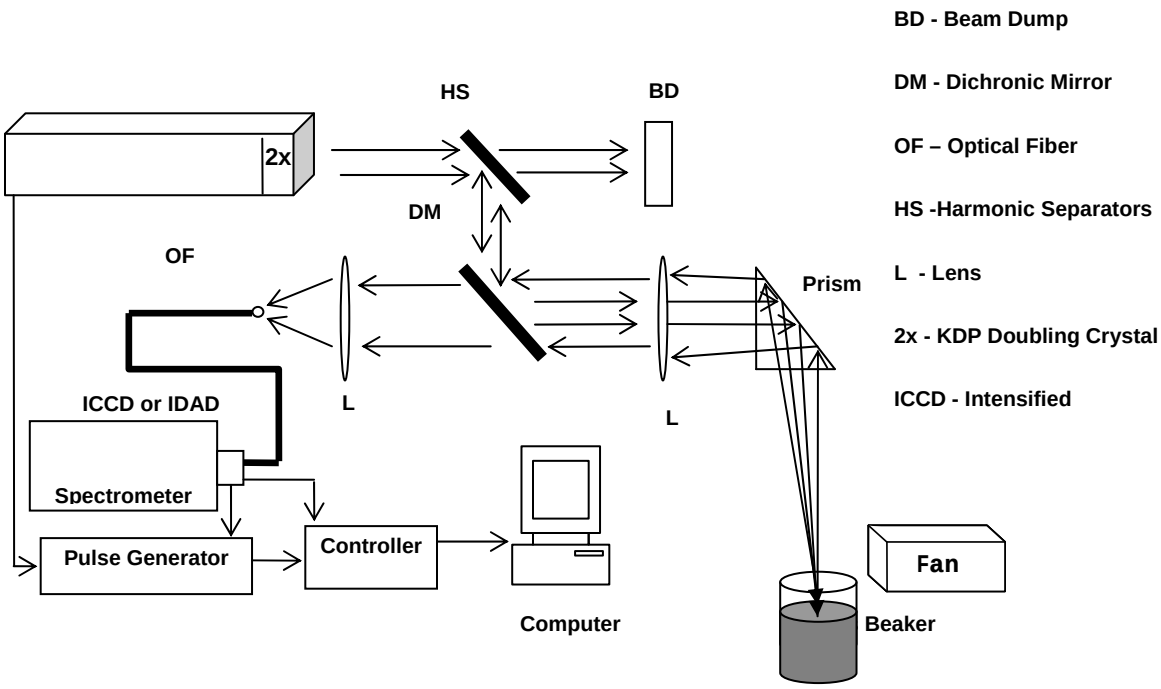

Figure 1. Schematic diagram of LIBS measurement apparatus.

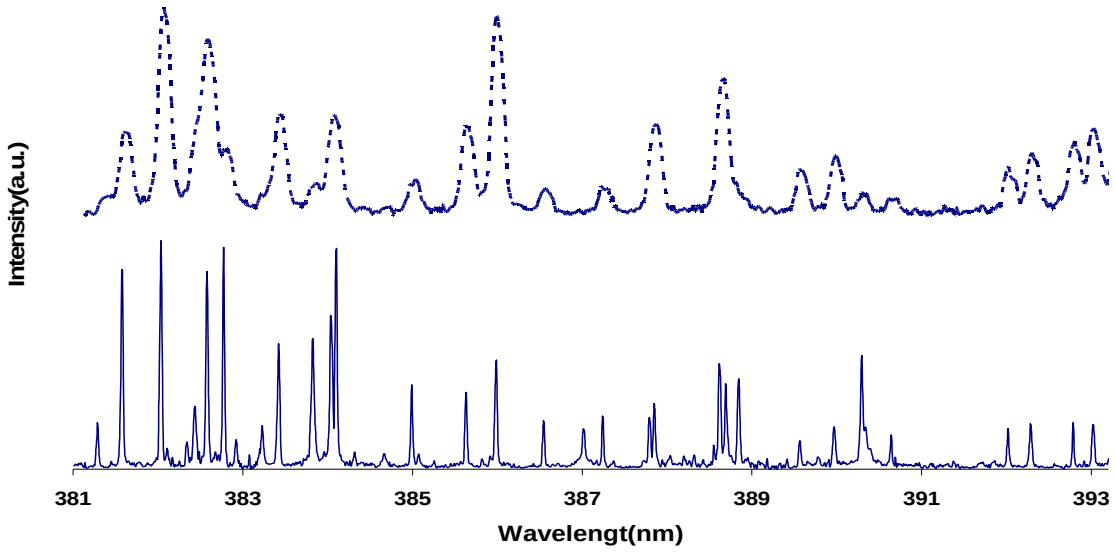

Figure 2. LIBS spectra of stimulant SRAT slurry around 386 nm. The spectra of dashed line and solid line are recorded by SPEX 500M and Echelle spectrometers, respectively.

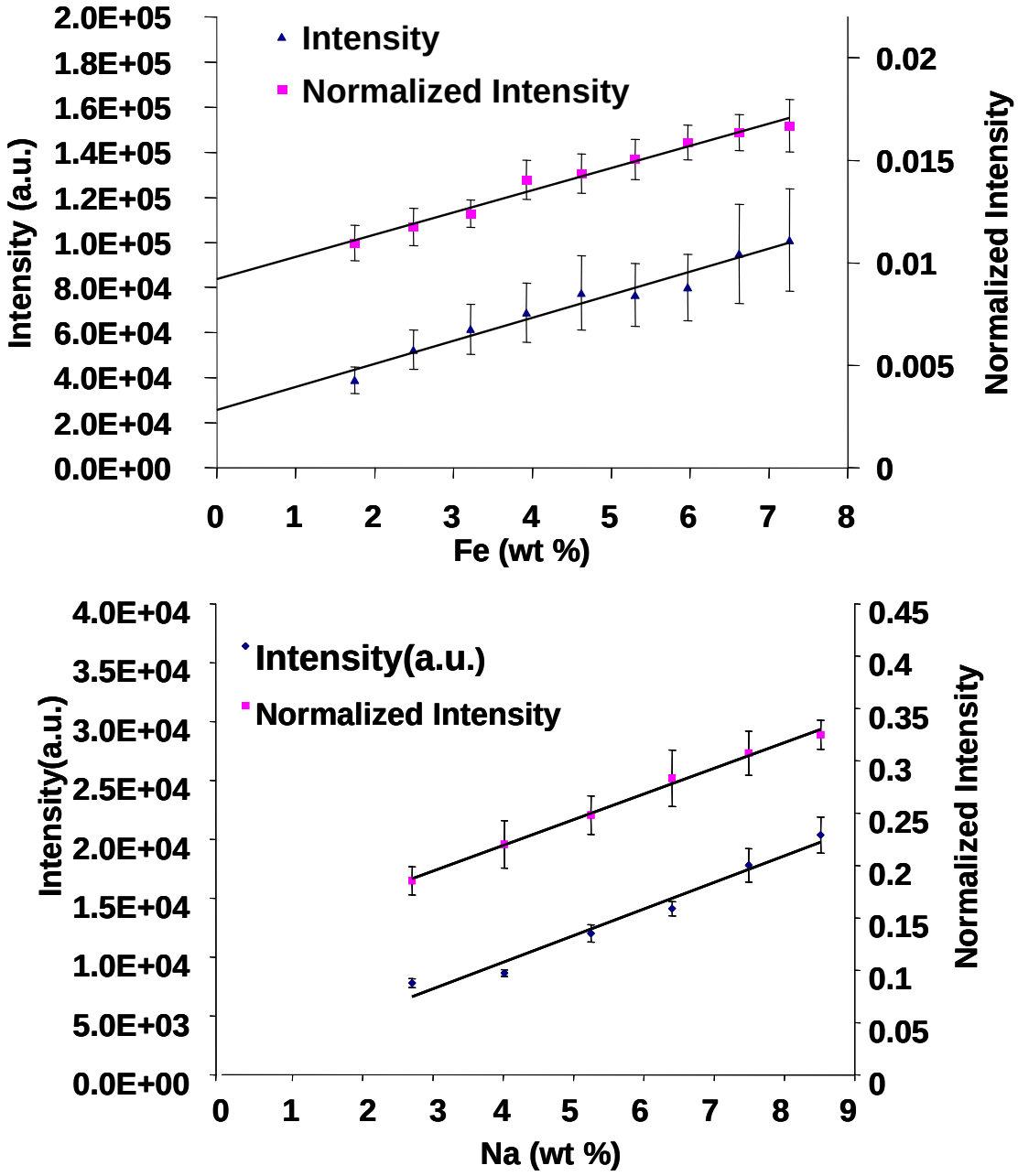

Figure 3. Calibration curves for Fe I 387.857nm line (top) and Na I 330.2 nm doublet line (bottom) recorded by the Czerny-Turner spectrometer system (SPEX 500M).

(a)

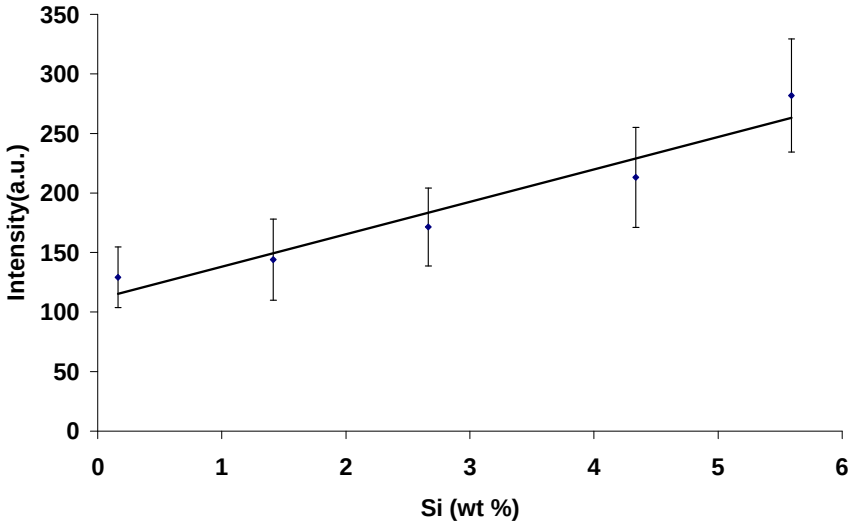

(b)

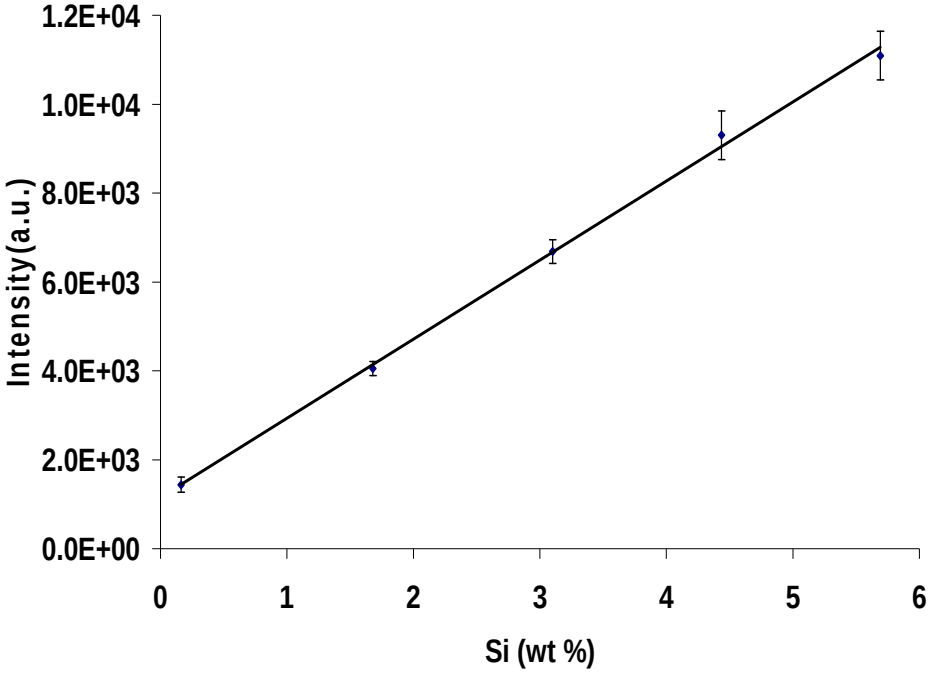

Figure 4. Calibration curve for Si I 288.158 nm line (a) using glass frit (70 mJ/pulse, gate delay 1μs and width 4 μs) and (b) using Silicon dioxide (SiO_2) (80 mJ/pulse, gate delay 300 ns and width 4 μs).

Table 1. Instrument information for two different LIBS systems

Detection System	Czerny-Tuner	Echelle
Spectrometer Model	Spex 500M	ESA 3000 LLA
Spectral Coverage	0-750 nm	200-780nm
Simultaneous Spectral range	~20nm	~580nm
Grating	2400 lines/mm	
Pulse Generator	Princeton Inst. PG-10	Fast pulse generator (Model 3000 FP)
ICCD or IDPA	EG&E PARC Model 4456 IDAD	KAF-1000 Kodak ICCD
Data Acquisition Software	OMAVISION	ESAWIN